Electric-field Bit Write-in for Molecular Quantum-dot Cellular Automata Circuits

Jackson Henry, Joseph Previti, and Enrique P. Blair, member, IEEE
Electrical and Computer Engineering Department
Baylor University
Waco, Texas 76798, United States of America
Email: Enrique_Blair@baylor.edu

***Abstract*—Quantum-dot cellular automata (QCA) was conceptualized to provide low-power, high-speed, general-purpose computing in the post-CMOS era. Here, an elementary device, called a "cell" is a system of quantum dots and a few mobile charges. The configuration of charge on a cell encodes a binary state, and cells are networked locally using the electrostatic field. Layouts of QCA cells on a substrate provide non-von-Neumann circuits in which digital logic, interconnections, and memory are intermingled. QCA supports reversible, adiabatic computing for arbitrarily low levels of dissipation. Here, we focus on a molecular implementation of QCA and describe the promise this holds. This discussion includes an outline of an architecture for clocked molecular QCA circuits and some technical challenges remaining before molecular QCA computation may be realized. This work focuses on the challenge of using macroscopic devices to write-in bits to nanoscale QCA molecules. We use an electric field established between electrodes fabricated using standard, mature lithographic processes, and the field need not feature single-molecule specificity. An intercellular Hartree approximation is used to model the state of an N-molecule circuit. Simulations of a method for providing bit inputs to clocked molecular circuits are shown.**

I. Introduction

The design and operation of transistors at the physical limits of scaling has led to significant power dissipation [1], the real and very present limit to progress. Present fabrication technologies support device densities of over 10^9 cm^{-2}, but full device utilization will dissipate levels of heat that can destroy the chip. While design techniques such as multi-core processors and dark silicon mitigate actual levels of dissipation, the ability to sink this heat dissipation has limited commercial computer clock speeds to 3-4 GHz since 2003. Additionally, power dissipation contributes directly to the significant and growing percentage of global electrical power consumed by information and computing technologies, calculated at 10% in 2010 and estimated to reach 30-50% in 2030 [2]. Clearly, to achieve energy-efficient, next-generation computing technologies, solutions beyond CMOS must be considered.

To answer the concerns raised by power dissipation in CMOS, a low-power, general-purpose, digital computational paradigm known as quantum-dot cellular automata (QCA) was developed [3]. In particular, a molecular implementation of QCA promises nanometer-scale devices [4]–[6], THz-or-faster switching speeds [7], and room-temperature operation. While QCA devices have been fabricated [8] and the concept of information processing using QCA circuits has been established [9], [10], technical challenges persist in the realization of molecular QCA.

In this paper, we provide simulations as *in silico* demonstrations of a technology for writing bits to nanoscale molecular QCA circuits. The discussion begins with Section II, which provides a brief overview of the QCA concept and emphasizes the molecular implementation. The concept of clocking in molecular QCA circuits is presented. The conclusion to Section II sets the context for our work by briefly overviewing the technical challenges which must be overcome if computation using molecular QCA is to be achieved, including: molecule design; molecular QCA circuit layout; bit inputs to the QCA molecules; and bit readout from molecular QCA circuits. In particular, own work proposes a solution for bit inputs to clocked molecular QCA circuits using electrodes which may be fabricated using mature nanolithographic processes. Section III describes the model used for describing a QCA circuit immersed in an electric field $\vec{E}\,(\vec{r})$ which provides both bit inputs and clocking. Simulation results of bits selected on clocked molecular QCA circuits are presented in Section IV. This solution for bit write-in is important because it may enable the experimental demonstration of controlled switching of QCA molecules, which in turn, will support the development and testing bit read-out technologies. This discussion is concluded in Section V by underscoring the fact that novel solutions to one technical challenge in realizing molecular QCA can help enable solutions to other challenges.

II. Overview of QCA

In QCA, the elementary device is a *cell*, a structure with a set of quantum dots which provide charge localization sites for a few mobile charges. The configuration of charge on these dots encodes a bit, and device switching occurs via the quantum tunneling of charge between the dots.

Fig. 1 depicts three states of a cell with six dots and two mobile electrons. The two states, labeled "0" and "1" are designated active states, and the third state is designated as "Null," conveying no information. The cell can be clocked to the Null state by applying a positive voltage sufficient to attract the electrons to the central null dots (dots 2 and 5). We refer to dots 1, 3, 4, and 6 as active dots. For this cell, it is

a design feature that direct tunneling between "0" and "1" is suppressed: the transition between either of the active states requires an intermediate transition to the "Null" state.

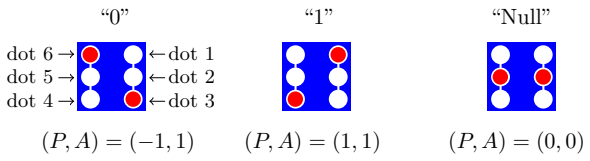

Fig. 1. Charge-localized states of a six-dot QCA cell. Two mobile electrons (red discs) provide three states on a system of six quantum dots (white discs). The thin, white connecting lines between dots indicate tunneling paths. Thus, a transition between the "0" and "1" states requires an intermediate transition to the "Null" state.

When arranged on a substrate, neighboring cells are networked locally via the electrostatic field, enabling general-purpose computation. Basic QCA circuits are shown in Fig. 2. Cells arranged in a row tend to align via simple Coulomb repulsion, and diagonal coupling can be used to achieve a bit inversion. The natural logic gate in QCA is the majority gate, for which three inputs have each an equal influence over a device cell. The bit in the majority on the inputs appears on the device cell and is copied to the output. Any one of the three inputs can function as a control bit, making the majority gate function as a programmable two-input AND/OR gate between the other two inputs. These devices provide a logically-complete set, from which more complex devices may be formed. QCA circuits such as adders and a Simple-12 processor have been designed [9], [10].

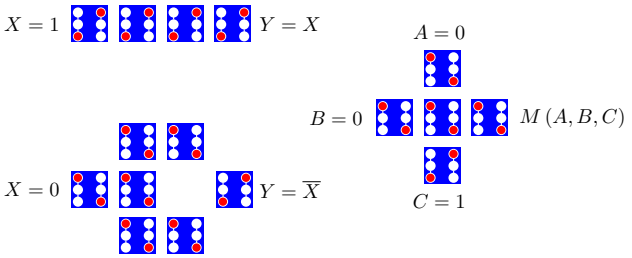

Fig. 2. Basic QCA devices. ***Upper left:*** cells arranged in a row function as a binary wire, as cells align through Coulomb repulsion. ***Lower left:*** diagonal interactions between cells provide a bit inversion. ***Right***: a majority gate has three inputs, A, B, and C, which vote on the state of the central device cell. $M(A, B, C)$ is the bit in the majority among the inputs, which appears on the device cell and gets copied to the ouput. One of inputs may be used as a control bit to program the gate to function as a programmable, two-input AND/OR gate between the other two inputs.

A. Molecular QCA

There are various implementations for QCA. The earliest implementation of QCA used metallic dots patterned on an insulating substrate [8], [11]. Here, tunnel junctions allow inter-dot charge transfer. Later, semiconductor quantum dots were used [12], [13]. Also, cells have been written on a hydrogen-passivated silicon surface using a scanning tunneling microscope (STM) tip: individual H atoms were removed, exposing single dangling bonds, each of which functions as a dot [14]. By virtue of nanometer-scale dimensions, these atomic-scale QCA cells have bit energies of the electron-volt scale and are robust at room temperature. Molecular QCA also support room-temperature operation and are the focus of this paper. Here, mixed-valence molecules function as QCA cells, and redox centers on those molecules provide dots [5], [6]. Molecular QCA also may support THz-scale or better device operation [7].

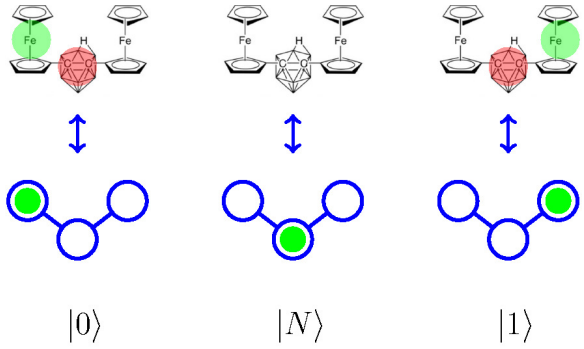

Fig. 3. A zwitterionic nido carborane ($Fc^+FcC_2B_9^-$) molecule is designed to function as a three-dot QCA cell. Two iron centers and one central carborane cage provide one quantum dot each. Three charge configurations of $Fc^+FcC_2B_9^-$ are depicted in the top row of this figure. When one mobile hole (translucent green disc) occupies the either iron center, it uncovers one electron (translucent red disc) on the central (null) dot. These are the active states "0" ($|0\rangle$) or "1" ($|1\rangle$). In the "Null" state ($|N\rangle$), the hole occupies the carborane cage, masking the fixed electron. The states of three-dot molecule are shown schematically in the bottom row of this graphic (the fixed electron is not shown).

The zwitterionic nido carborane molecule ($Fc^+FcC_2B_9^-$) was designed specifically for use as a QCA molecule [15]. $Fc^+FcC_2B_9^-$ is a self-doping molecule with a net-zero charge which provides three dots, as shown in Fig. 3. In $Fc^+FcC_2B_9^-$, the mobile charge is a single hole. Two such molecules can be paired to function as a six-dot QCA cell like the one depicted in Fig. 1.

A key advantage of molecular QCA is the small length scale of molecular cells. This length scale enables ultra-high device densities at 10^{14} cm^{-2} for tight-packed, 1-nm cells. The molecular QCA length scale also provides bit energies robust at room temperature. Consider a pair of two-dot QCA molecules of length a, separated by distance a, as shown in Fig. 4. We define the kink energy, E_k, as the cost of a bit flip. This is the difference in electrostatic energy between the kinked configuration of two cells [Fig. 4(b)] and their relaxed (favored) configuration [Fig. 4(a)]. It can be shown that the kink energy depends on the length a of the cells and physical constants ϵ_0 (the permittivity of free space), q (the fundamental charge):

$$E_k = \frac{q^2}{4\pi\epsilon_0 a}\left(1 - \frac{1}{\sqrt{2}}\right) . \qquad (1)$$

The kink energy also defines the bit energy for the double-dot QCA cell. Eqn. (1) also holds for three-dot QCA cells.

Fig. 5 shows that the length scale of molecular QCA allows E_k to be much greater than thermal noise k_BT at terrestrial

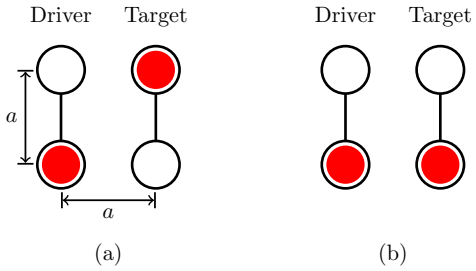

Fig. 4. The bit energy for a molecular two-dot cells is the kink energy, the difference in electrostatic energies of the two-cell favored configuration [subfigure (a)] and the kinked congfiguration [subfigure (b)], given that the driver is fixed as shown.

temperatures, where k_B is Boltzmann's constant, and $T = 300$ K. For molecules as small as $a = 0.7$ nm, $E_k \sim 20 k_B T$. On the other hand, lithographic QCA support length scales of $a \sim 10$ nm for bit energies of $E_k \sim k_B T$.

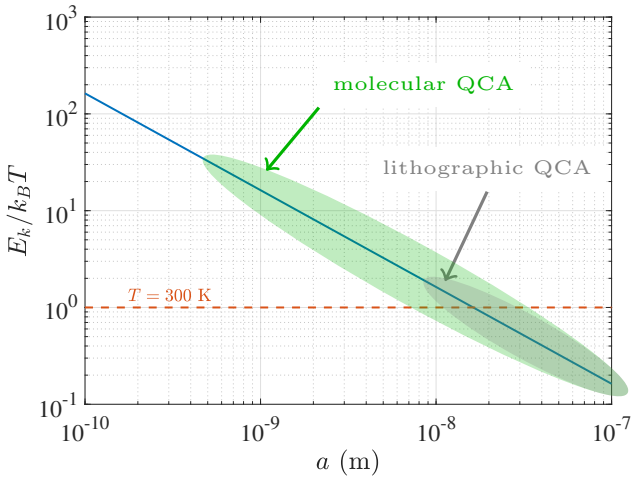

Fig. 5. Molecular QCA support room-temperature operation, because with feature sizes of ~ 1 nm, QCA molecules allow bit energies (E_k) that are much larger than thermal noise $k_B T$ at room temperature ($T = 300$ K). On the other hand, for lithographically-fabricated cells (metal-dot or semiconductor-dot QCA), feature sizes are ~ 10 nm, for which $E_k \sim k_B T$ for terrestrial T. Cryogenic temperatures are required for robust circuit operation in lithographic implementations.

B. Clocked Molecular QCA

Molecular six-dot cells may be clocked using an externally-applied electric field [16], as depicted in Fig. 6. Here, the six-dot cell is attached to the substrate by the null dots, so that the active dots are elevated above the substrate. A voltage applied to a conducting slab buried beneath the molecule results in an electrostatic field with a vertical component that affects the state of the cell. In this depiction, the mobile charge is a pair of electrons, so that a negative voltage applied to the slab repels the electrons from the null dots, forcing the cell to take an active state determined by interaction with neighboring cells. A positive clocking voltage, on the other hand, establishes an electric field which attracts the mobile electrons to the null dots, and the cell takes the null state regardless of neighbor interactions. Since direct tunneling between active states is suppressed, clocked molecular QCA support latching. Once the cell is clocked to an active state X, it is latched in X until the clock is lowered: a bit flip $X \rightarrow \overline{X}$ first requires a reset to the null state, which is prevented by the clock.

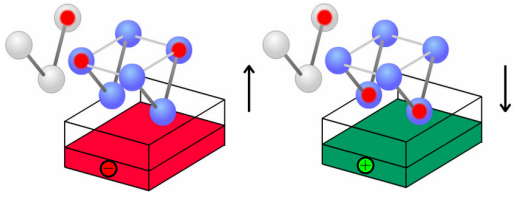

Fig. 6. A molecular six-dot cell is clocked using an externally-applied electric field. Light-blue spheres represent the quantum dots of a six-dot cell, and a red sphere represents a single mobile electron. The cell is adsorbed onto the substrate at the central ("null") dots such that the active dots used to represent "0" and "1" are elevated above the substrate. An electric field with a vertical component can be applied to the molecule using a buried conducting slab. A negative voltage establishes a field that repels the mobile electrons from the null dots. With this bias, the cell is forced to the active state favored by neighbor interactions. A positive voltage, on the other hand, attracts the electrons to the null dots so that the cell takes the null state regardless of the states of neighboring molecules.

Arrays of independently-charged conductors can be used to create an inhomogeneous electric at the device layer, as shown in Fig. 7. Some domains of the field activate cells; other regions clock cells to the null state. Calculations will take place in the transition region between active and null domains. It is worth noting that the clocking conductors may be much larger than the molecules themselves. QCA molecules are of the 1-nm scale, and it would be onerous if not intractable to wire each individual molecule, a task that this clocking scheme avoids.

Calculations become dynamic when the excitation applied to the clocking wires is time-dependent. Consider the plan view of buried clocking wires shown in Fig. 8. Here, an array of parallel clocking wires is laid out like ties supporting a railroad track. A four-phase voltage is applied to this set of wires, resulting in a time-varying electric field at the device layer with active domains which propagate rightward along the track. A calculation of $E_z(\vec{r})$ (pointing out of the page) at the device plane is visualized in the lower part of Fig. 8.

Fig. 9 demonstrates how active domains from the field of Fig. 8 can be used to drive bit packets through circuitry. Here, we zoom in from the length scale of the clocking wires (100 nm in length) to the length scale of several cells (each cell is a 1-nm-by-1-nm square) to see an active domain propagating along a binary wire. The strong clocking field at the center of the active domain has latched cells in a given state. Cells at the leading edge of the active domain are activated to the state favored by interactions with their latched neighbors to their immediate left (more internal to the active domain). Computation—in this case, a bit copy—occurs at the leading edge of the moving active domain. At the trailing edge of the active domain, cells are released to the null state in preparation

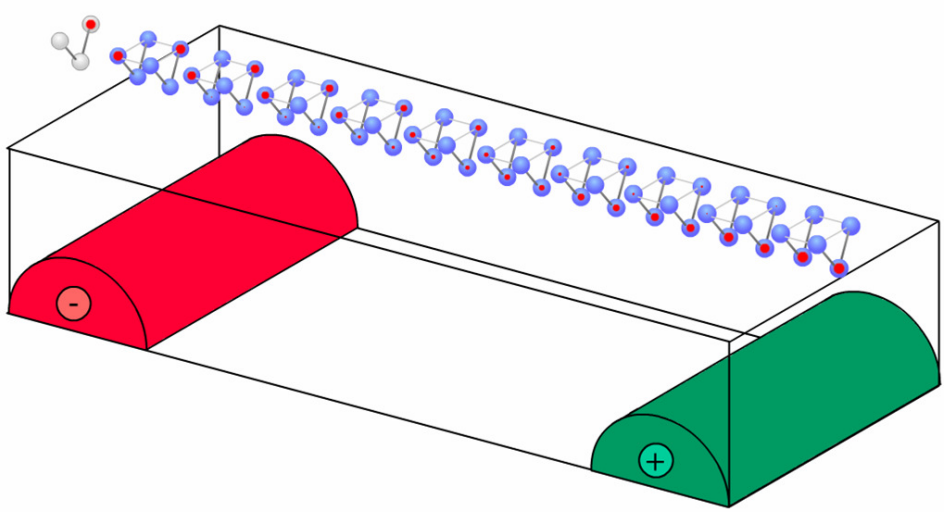

Fig. 7. Multiple indpendently-charged conductors can establish an electric field with an inhomogeneous vertical component at the QCA device plane. In some domains of this field, cells will be driven to active states, whereas in other regions, cells will be driven to the null state. Calculations and erasures will occur in the transitions between active and null domains.

for another computation. Since the action of the binary wire is clocked rather than ballistic, we refer to this as a shift register. Computations may be more complex than a mere copy, however: logic gates such as AND, OR, NOT, and XOR have been simulated.

In this clocking paradigm for molecular QCA, clock parameters determine circuit operation. For example, the frequency of the clock signal determines the number of calculations driven through a particular circuit per unit time. The pitch of the clocking conductors will determine the wavelength of the clock, or the length of the active domains. The amplitude of the clocking voltage along with any DC bias applied will determine the strength of active and null domains.

C. Realizing Molecular QCA Computation

Technical challenges remain in the path to realizing molecular QCA. We briefly outline these challenges here, and discuss the state of solutions to these challenges. Technical challenges include:

1) **Molecule design.** The design of QCA molecules is an ongoing endeavor involving physicists, synthetic chemists, and physical chemists. New molecules are being designed and studied as QCA candidates [15], [17]. Models are being developed to predict the performance of molecules as QCA devices. Such predictive models must treat relevant quantum phenomena for particular QCA candidates such as electron localization and the self-trapping of charge [18]–[20], vibration-coupled electron transfer [7], as well as environmentally-driven quantum decoherence [21], [22], power dissipation, and disentanglement [23]. Candidate molecules may be functionalized with a ligand to facilitate adsorption on a substrate.

   Some helpful advances have come from this work. The development of net-neutral, self-doping QCA candidate molecules [15] eliminate the need for additional counterions associated with each cell. Theoretical work suggests that environmental interactions strengthen molecular QCA bits [21]. Models of field-driven, vibration-coupled electron transfer suggest QCA can switch at THz or faster speeds [7].

   Controlled switching has not yet been observed in any molecule. Thus, efforts on designing, synthesizing, and testing individual molecuar QCA species will be efforts well-spent. Models of circuit-level behaviors for particular molecular species may also be developed.

2) **Circuit layout.** The layout of molecular circuitry is another technical challenge. Homogenous monolayers of devices, while the most simple to achieve, perform no useful calculation. Therefore, the preferential layout of molecules in well-defined, specific arrangements is necessary.

   For circuit layout, self-assembled techniques are promising. Researchers have demonstrated exquisite control over processes to form 2D and 3D structures from DNA [24], [25]. In particular, DNA tiles may be used as molecular circuit boards [26]. Here, DNA tiles will be programmed with specific sites to conjugate with a docking ligand built into the QCA molecule. It may be possible to control the location of DNA tiles on a substrate using lithographic techniques.

   One challenge with DNA tiles is localized negative charges due to phosphate groups on the DNA itself. Stray charge has been shown to adversely affect the performance of QCA devices [27], [28]. Therefore, tiles formed from pep-

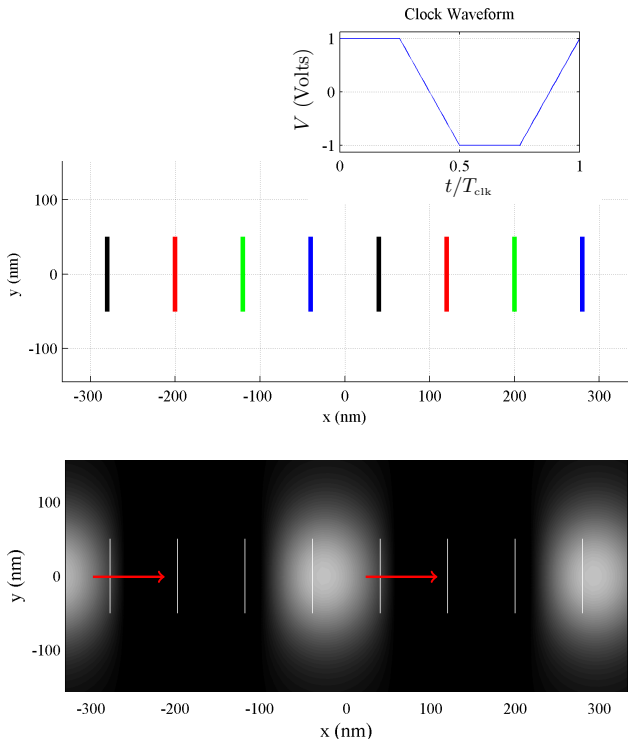

Fig. 8. A four-phase voltage is applied to an array of wires to create a time-dependent, inhomogeneous clocking electric field. ***Middle:*** a plan view of a layout of clocking wires is shown. Wires (colored lines) are laid out in parallel, like railroad ties. A four-phase voltage is applied to these wires, and the color of each wire indicates one of the four particular voltage phases. ***Upper right:*** one phase of the four-phase clocking voltage is shown here, with clock period T_{clk}. ***Bottom:*** E_z, the $\hat{z}$-component (coming out of the page) of the electric field at the device layer is coded in the grayscale background. White regions in E_z represent active domains, and black regions in E_z drive cells to the null state. White lines mark the position of clocking wires, and red arrows indicate that the active domains propagate rightward in time.

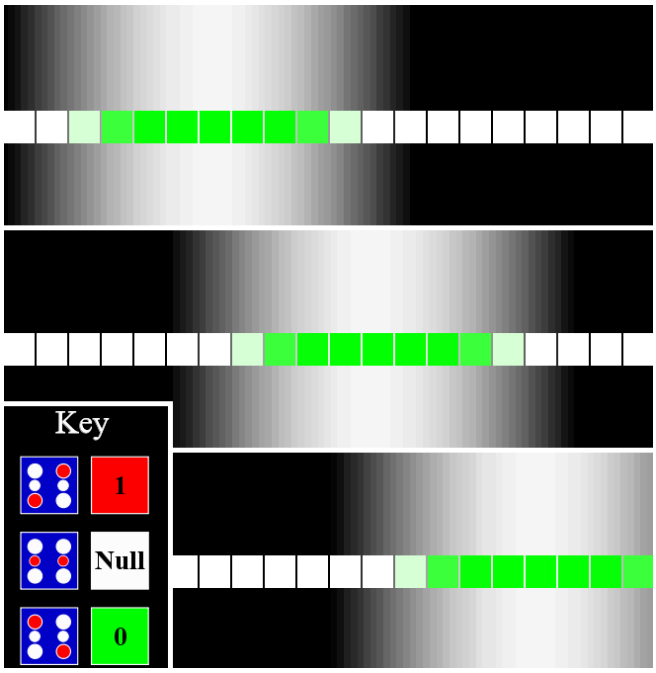

Fig. 9. An active domain in the clocking field E_z carries a "0" bit packet through a binary wire. Three time-ordered snapshots are shown of an active domain (white region of background grayscale gradient representing E_z) sweeping rightward along a binary wire (row of squares). The face color of each cells is coded to indicate its state, as shown in the inset labeled "Key"). As the active domain propagates rightward, the cells at the leading (right-most) edge of the active domain transition from "Null" to an active state determined by interaction with neighboring, latched cells deeper within the active domain. Cells at the trailing (left-most) edge of the active domain are released to the Null state. Here, a "0" bit was clocked from other cells to the left of the segment shown, and the output propagates rightward off the image. The action here is not ballistic, but rather is synchronous. Therefore, this is not just a binary wire, but also a shift register.

tide nucleic acid (PNA) [29] may better serve as molecular QCA circuit boards, since PNA has no such stray charge.

3) **Bit write-in for molecular circuits.** The nanometer scale of molecular QCA makes bit input more challenging than in conventional devices. It is neither possible nor desirable to form contacts that address individual molecules, because lithographically-feasible devices are an order of magnitude larger than molecular QCA. Optical control of molecular QCA is challenging because optical wavelengths are much longer than the length scale of desirable QCA molecules, and optical interactions are weak at this scale. Additionally, beam sizes are macroscopic, so they can only illuminate large groups of molecular QCA.
   Some solutions to the bit input problem have been proposed. One system proposed complementary pairs of fixed-state molecules as bit sources to a shift register [30]. The clock is used to selectively couple one of the sources to a binary wire. In addition to the molecular species required to implement the clocked molecular QCA, this solution likely requires the use of a second molecular species to provide the fixed input sources. Another concept modeled by by Pulimeno, *et al*, was an input electric field applied to a single molecule at the end of a row of clocked, three-dot bisferrocene molecules [31]. While this eliminates the need for fixed-state molecules, nanoelectrodes are required to generate a field with single-molecule specificity.
4) **Bit read-out from molecular QCA circuits.** One promising approach to the detection of the state of QCA molecules is the use of single-electron devices, such as single-electron transistors (SETs) [32] and single-electron boxes (SEB) [33]. In particular, SETs have demonstrated sensitivity to single-electron tunneling events over distances less than one nanometer [34]. SETs and SEBs require cryogenic temperatures for operation. The readout of molecular QCA states using SETs or SEBs has not yet been achieved. This will be enabled by the development of a method for controllably switching QCA molecules which is amenable to SET- or SEB-based read-out.

The focus of this paper is to present models of a solution for bit write-in to clocked molecular QCA circuits which requires neither fixed-state QCA molecules nor fields with single-molecule specificity. This extends an earlier work that proposed an input system for asynchronous molecular QCA

circuits, in which lithographically-formed electrodes establish an input field $\vec{E}_{in}$ to select the state of multiple unclocked two-dot molecules [35]. The selected input bit packet may then be transmitted via a binary wire to QCA circuitry for processing. It was shown that single-molecule specificity is not required of $\vec{E}_{in}$ for the input circuits to work; however, if the interaction of $\vec{E}_{in}$ with the binary wire portion can be suppressed, the circuits will be more robust.

III. Model for Bit Write-in to Molecular QCA Circuits

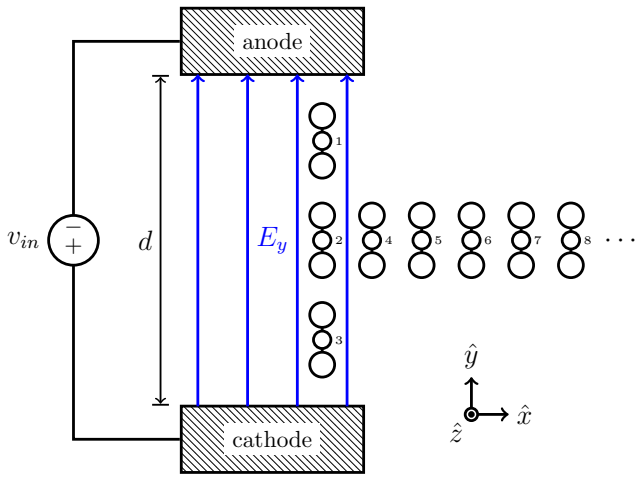

Fig. 10. An input voltage v_{in} is applied to electrodes to select a QCA input bit. Each three-dot QCA molecuis is schematically drawn as system of three quantum dots (black circles). The middle dot is drawn smaller than the other two to indicate that it sits on the substrate ($z = 0$), while the other dots are elevated above the substrate in the $+\hat{z}$ direction. Each cell is assigned the number next to its middle dot. The applied v_{in} establishes an electric field $\vec{E} = E_y\hat{y}$, which immerses the column of molecules aligned in the $\pm\hat{y}$ direction (cells 1-3). Thus, E_y will select the state of molecules 1-3, which are activated when a negative clock (the z-component, $E_z\hat{z}$) is applied. The row of molecules aligned in the $\pm\hat{x}$ direction (cells 4-8) will function as a shift register and can transmit the input bit to other QCA circuitry.

A clocked molecular QCA input circuit is depicted in Fig. 10. Here, we apply a constant field $\vec{E}(\vec{r}) = \vec{E}_{in} + \vec{E}_{clk}$. Input field $\vec{E}_{in}(\vec{r})$ selects bits on cells 1-3, and the field $\vec{E}_{clk}(\vec{r})$ for clockings the entire molecular circuit. The input field $\vec{E}_{in}$ is idealized to

$$\vec{E}_{in}(\vec{r}) = \begin{cases} E_y\hat{y}, & \text{in the volume between electrodes,} \\ 0, & \text{elsewhere,} \end{cases} \tag{2}$$

with

$$E_y = \frac{v_{in}}{d}\ . \tag{3}$$

Thus, present results are calculated within a limit where interaction between $\vec{E}_{in}$ and the shift register (cells 4-8) may be suppressed. The clock $\vec{E}_{clk}(\vec{r})$ is assumed to be uniform: $\vec{E}_{clk}(\vec{r}) = E_z\hat{z}$ over all space. Cells 4-8 shift the selected input bit to computational QCA circuits. With this approach, a single molecular species can provide both input devices and computational QCA circuits.

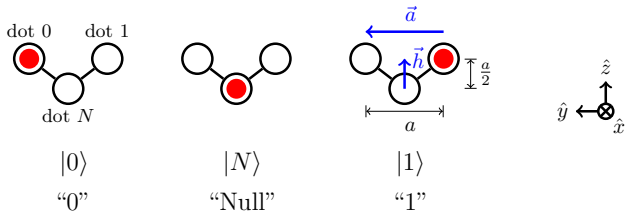

Fig. 11. The localized states $\{|0\rangle, \}$ of a mobile electron provide a basis state for a three-dot QCA molecule. The red disc represents one mobile electron. Neutralizing charge is not shown. Solid lines show tunneling paths between dots, so that tunneling occurs between dots 0 and N or dots 1 and N only (direct tunneling between dots 0 and 1 is suppressed). The orientation vectors indicate how the molecules are arranged in Fig. fig:FieldInputConcept: the dot 0 is on the substrate, and dots 0 and 1 are elevated above the substrate by $h = a/2$. The vector $\vec{a}$ points in the $+\hat{y}$-direction, and the vector $\hat{h}$ points in the $+\hat{z}$ direction for all cells.

A single three-dot molecule like $\mathrm{Fc}^{+}\mathrm{FcC_2B_9}^{-}$ is modeled as a quantum three-state system. Fig. 11 shows the localized states of a single mobile electron for this molecule. These states form a basis $\mathcal{B} = \{|0\rangle, |N\rangle, |1\rangle\}$ for the molecule's electronic quantum state. Here, $\vec{a}$ is a displacement vector from dot 1 to dot 0 of the cell, and $\vec{h}$ is a displacement from dot zero to a line passing through both dots 0 and 1 perpendicular to $\vec{a}$. All charges are treated as point charges.

The Hamiltonian for a single cell immersed in electrostatic electric field $\vec{E}$ may be written as

$$\hat{H} = \hat{H}_o + \hat{H}_E + \hat{H}_{\text{int}} \tag{4}$$

with

$$\hat{H}_o = -\gamma\left(\hat{P}_{1,N} + \hat{P}_{N,1} + \hat{P}_{0,N} + \hat{P}_{N,0}\right),$$

$$\hat{H}_E = -\frac{q_e\vec{E}\cdot\vec{a}}{2}\left(\hat{P}_{1,1} - \hat{P}_{0,0}\right) - q_e\vec{E}\cdot\vec{h}\hat{P}_{N,N}, \text{ and} \tag{5}$$

$$\hat{H}_{\text{int}} = \sum_{\substack{j\in\{0,N,1\} \\ l}} U_j^{(l)}\hat{P}_{j,j}. \tag{6}$$

Inter-dot electron transfers are described by $\hat{H}_o$, in which γ is the hopping energy and $\hat{P}_{j,k} \equiv |j\rangle\langle k|$ are transition operators. The projection operators $\hat{P}_{j,j} \equiv |j\rangle\langle j|$ are used to form $\hat{H}_E$, which includes the effects of the applied field. The first term of $\hat{H}_E$ describes the field-driven bias between the active states $|0\rangle$ and $|1\rangle$, and the second term describes the field-driven bias between $|N\rangle$ and the active states. Finally, $\hat{H}_{\text{int}}$ describes the interaction between the cell and any neighbors, each labeled with an integer $l \in \{1, 2, \ldots\}$. The electrostatic potential energy $U_j^{(l)}$ is calculated by setting the target cell to state $|j\rangle$ and then evaluating the electrostatic energy of interaction between the charges from neighbor l with the charges in the target cell. $U_j^{(l)}$ depends on the state of the l-th neighbor cell.

The ground state of a circuit of M cells maps to the desired calculational result. To calculate the ground state, an intercellular Hartree approximation (IHCA) is made [36]. This involves making an initial guess for the ground state of each cell in the M-cell circuit, and then iterating through the circuit,

relaxing each cell to its ground state. This process is repeated until a self-consistent configuration is achieved for the circuit.

IV. Results

A simulation of a clocked QCA input system of Fig. 10 is shown in Fig. 12. Specifying a bit on the input cells is a matter of specifying the sign of E_y of an appropriate magnitude and then applying a clock voltage $\vec{E}_{clk} = E_z\hat{z}$. The field is specified in units of E_o, the input field strength required to induce a kink between two molecules:

$$E_o = \left| \frac{E_k}{q_e a} \right| . \tag{7}$$

Here, even an input field $E_y < E_o$ is sufficient to select an input bit, and an applied clock $E_z = -1.5E_o$ activates the system of cells. In this case, cells 1 and 3 could be eliminated; however, they are necessary in the case where $\vec{E}_{in} = E_y\hat{y}$ is uniform and is applied to all cells (molecules 1-8) (see [35]). Cells 1 and 3 also may be helpful when fringing field effects are considered. These results were calculated using an IHCA approach with only nearest-neighbor and next-nearest neighbor interactions.

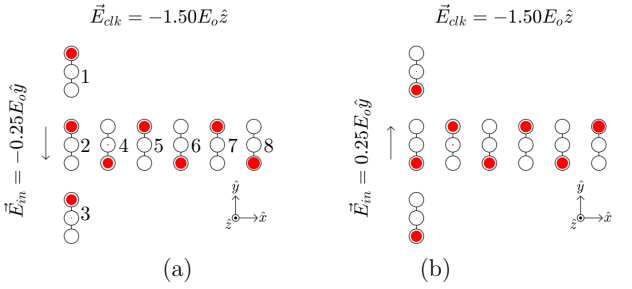

Fig. 12. An applied electric field $\vec{E} = \vec{E}_{in} + \vec{E}_{clk}$ selects an input state and activates the circuit. The input field $\vec{E}_{in} = E_y\hat{y}$ is applied across cells 1-3 only. Subfigure (a): for an input field $E_y < 0$, cells in this column take the $|0\rangle$ state. Subfigure (b): when $E_y > 0$, cells in this column take the $|1\rangle$ state. In each case, the binary wire formed by cells 4-8 couples to the input cells (cells 1-3), and the bit propagates rightward from the input to other QCA circuits beyond cell 8.

The result of Fig. 12 is extended simply to a simulated ground state for a majority gate, shown in Fig. 13. Here, three separate bit inputs are supplied to a majority gate, and the two majority bits dominate the minority bit.

While this demonstrates *in silico* the viability of clocked majority logic using three-dot molecules, a more realistic simulation of the electrode/molecular-circuit input system requires further development of the model's software implementation. A larger circuit footprint would be required to accommodate large input electrodes, and the majority logic will likely require isolation from fringing fields due to input electrodes. This will require longer shift registers between inputs and the majority gate. A larger circuit with more molecules will likely require a non-uniform, time-dependent clock $\vec{E}_{clk}(\vec{r}, t)$.

More detailed explorations of molecular QCA input systems are needed. Some modifications to the molecular input

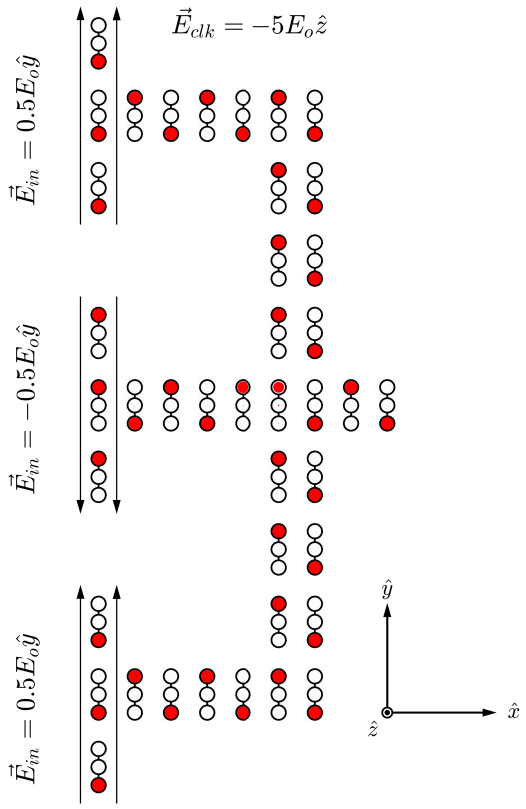

Fig. 13. A clocked molecular majority gate is a simple extension of the input circuit from Fig. 12. Here, two like bits dominate one unlike bit in a majority circuit.

circuitry could provide a more robust response. Fringing-field effects should be considered, and an inhomogeneous, time-dependent clock field $\vec{E}_{clk}(\vec{r}, t)$ may be designed to optimize circuit performance, along with a time-dependent, inhomogeneous input field $\vec{E}_{in}(\vec{r}, t)$. This will be necessary to better isolate logic from input fields, and it will require further development of the software implementing our model.

V. Conclusion

Molecular QCA is a promising candidate for post-CMOS computation because this paradigm can provide high operating speeds, high device densities, and low power dissipation. In order to realize molecular QCA computation, some strategic advances are required in molecular design, synthesis and testing; circuit layout; and bit input and readout. Solutions to these technical challenges have been conceived, and, with some strategically focused effort, these challenges may be overcome.

In this paper, an input system for clocked, molecular three-dot QCA cells has been introduced, and simple calculations for this system are provided. This system does not require fixed-state input molecules, which would necessitate a separate species of molecule in addition to the computational molecules. This input system may be achieved using electrodes easily fabricated using mature photolithographic processes.

Only a uniform clocking field was considered here, and fringing input fields were neglected. Present efforts and future work will focus on developing the software implementation of the model to support less-idealized fields.

The work presented here is focused on addressing the challenge of bit write-in for molecular QCA. This solution could provide insights into as well as helpful constraints for solutions to other challenges. This input concept may prove useful in enabling the demonstration of controlled switching in QCA molecules, as well as the read-out of QCA molecules using SETs or SEBs. Additionally, the features of the proposed input system may also identify capabilities desirable in a solution to the problem of molecular circuit layout.

It is our hope that discussions such as the one presented here can inspire dialog and collaborations between diverse groups of researchers and help advance the field of QCA computation closer to realization.

ACKNOWLEDGMENT

J.H. is responsible for simulation and modeling; J.P. contributed to the development of a layout/design tool for clocked molecular circuits; and E.B. supervised and directed this project, and drafted the manuscript. This research was supported under a new-faculty-start-up grant from Baylor University. The author thanks C.S. Lent and G.L. Snider of the University of Notre Dame for insightful discussion.

REFERENCES

[1] D. Frank, "Power-constrained cmos scaling limits," *IBM J Res Dev*, vol. 46, no. 2/3, pp. 235–244, March/May 2002.

[2] A. Andrae and T. Edler, "On global electricity usage of communication technology: Trends to 2030," *Challenges*, vol. 6, pp. 117–157, 2015.

[3] C. Lent, P. Tougaw, W. Porod, and G. Bernstein, "Quantum cellular automata," *Nanotechnology*, vol. 4, p. 49, 1993.

[4] C. S. Lent, "Molecular electronics - bypassing the transistor paradigm," *Science*, vol. 288, pp. 1597–1599, Jun. 2000.

[5] M. Lieberman, S. Chellamma, B. Varughese, Y. Wang, C. Lent, G. Bernstein, G. Snider, and F. Peiris, "Quantum-dot cellular automata at a molecular scale," *Ann. N.Y. Acad. Sci.*, vol. 960, pp. 225–239, 2002.

[6] C. Lent, B. Isaksen, and M. Lieberman, "Molecular quantum-dot cellular automata," *J. Am. Chem. Soc.*, vol. 125, pp. 1056–1063, 2003.

[7] E. Blair, S. Corcelli, and C. Lent, "Electric-field-driven electron-transfer in mixed-valence molecules," *J Chem Phys*, vol. 145, p. 014307, June 2016.

[8] A. O. Orlov, I. Amlani, G. H. Bernstein, C. S. Lent, and G. L. Snider, "Realization of a functional cell for quantum-dot cellular automata," *Science*, vol. 277, no. 5328, pp. 928–930, Aug. 1997.

[9] P. Tougaw and C. Lent, "Logical devices implemented using quantum cellular automata," *J. Appl. Phys.*, vol. 75, no. 3, pp. 1818–1825, Feb. 1994.

[10] M. Niemier, M. Kontz, and P. Kogge, "A design of and design tools for a novel quantum dot based microprocessor," in *Proc. of the 37th Design Automation Conf.*, 2000, pp. 227–232.

[11] I. Amlani, A. Orlov, G. Snider, and C. Lent, "Demonstration of a six-dot quantum cellular automata system," *Appl. Phys. Lett.*, vol. 72, pp. 2179–2181, 1998.

[12] C. Smith, S. Gardelis, A. Rushforth, R. Crook, J. Cooper, D. Ritchie, E. Linfield, Y. Jin, and M. Pepper, "Realization of quantum-dot cellular automata using semiconductor quantum dots," *SUPERLATTICES AND MICROSTRUCTURES*, vol. 34, no. 3-6, pp. 195–203, SEP-DEC 2003, 6th International Conference on New Phenomena in Mesoscopic Structures/4th International Conference on Surfaces and Interfaces of Mesoscopic Devices, Maui, HI, DEC 01-05, 2003.

[13] S. Gardelis, C. Smith, J. Cooper, D. Ritchie, E. Linfield, and Y. Jin, "Evidence for transfer of polarization in a quantum dot cellular automata cell consisting of semiconductor quantum dots," *PHYSICAL REVIEW B*, vol. 67, no. 3, JAN 15 2003.

[14] M. B. Haider, J. L. Pitters, G. A. DiLabio, L. Livadaru, J. Y. Mutus, and R. A. Wolkow, "Controlled coupling and occupation of silicon atomic quantum dots at room temperature," *Phys. Rev. Lett.*, vol. 102, p. 046805, 2009.

[15] J. Christie, R. Forrest, S. Corcelli, N. Wasio, R. Quardokus, R. Brown, S. Kandel, Y. Lu, C. Lent, and K. Henderson, "Synthesis of a neutral mixed-valence diferrocenyl carborane for molecular quantum-dot cellular automata applications," *Angewandte Chemie*, vol. 127, pp. 15 668–15 671, 2015.

[16] K. Hennessy and C. S. Lent, "Clocking of molecular quantum-dot cellular automata," *Journal of Vacuum Science & Technology B*, vol. 19, no. 5, pp. 1752–1755, Sep. 2001.

[17] R. Quardokus, N. Wasio, R. Forrest, C. Lent, S. Corcelli, J. Christie, K. Henderson, and S. Kandel, "Adsorption of diferrocenylacetylene on au(111) studied by scanning tunneling microscopy," *Phys. Chem. Chem. Phys.*, vol. 18, pp. 6973–6981, 2013.

[18] Y. Lu, R. Quardokus, C. Lent, F. Justaud, C. Lapinte, and S. Kandel, "Charge localization in isolated mixed-valence complexes: an stm and theoretical study," *J. Am. Chem. Soc.*, vol. 132, no. 38, pp. 13 519–13 524, 2010.

[19] B. Tsukerblat, A. Palii, and J. Clemente-Juan, "Self-trapping of charge polarized states in four-dot molecular quantum cellular automata: bi-electronic tetrameric mixed-valence species," *Pure and Applied Chemistry*, vol. 87, no. 3, pp. 271–282, 2015.

[20] J. Henry and E. Blair, "The role of the tunneling matrix element and nuclear reorganization in the design of quantum-dot cellular automata molecules," *J Appl Phys*, vol. 123, no. 6, p. 064302, 2018.

[21] E. P. Blair and C. S. Lent, "Environmental decoherence stabilizes quantum-dot cellular automata," *J. Appl. Phys.*, vol. 113, p. 124302, JAN 2013.

[22] J. S. Ramsey and E. P. Blair, "Operator-sum models of quantum decoherence in molecular quantum-dot cellular automata," *J Appl Phys*, vol. 122, p. 084304, August 2017.

[23] E. Blair, G. Toth, and C. Lent, "Entanglement loss in molecular quantum-dot qubits due to interaction with the environment," *Journal of Physics: Condensed Matter*, vol. 30, no. 19, p. 195602, 2018.

[24] E. Winfree, F. Liu, L. Wenzler, and N. Seeman, "Design and self-assembly of two-dimensional dna crystals," *Nature*, vol. 349, pp. 539–544, 1998.

[25] P. Rothemund, "Folding dna to create nanoscale shapes and patterns," *Nature*, vol. 440, pp. 297–302, 2006.

[26] K. Sarveswaran, P. Huber, M. Lieberman, C. Russo, and C. Lent, "Nanometer scale rafts built from dna tiles," in *PROCEEDINGS OF THE THIRD IEEE CONFERENCE ON NANOTECHNOLOGY (IEEE NANO 2003)*, 2003, pp. 417–420.

[27] P. Tougaw and C. Lent, "The effect of stray charge on quantum cellular automata," *Jpn. J. Appl. Phys.*, vol. 34, pp. 4373–4375, 1995.

[28] M. LaRue, D. Tougaw, and J. Will, "Stray charge in quantum-dot cellular automata: A validation of the intercellular hartree approximation," *IEEE Trans Nanotechnol*, vol. 12, no. 2, pp. 225–233, 2013.

[29] P. Nielsen, M. Egholm, R. Berg, and O. Buchardt, "Sequence-selective recognition of dna by strand displacement with a thymine-substituted polyamide," *Science*, vol. 254, no. 5037, pp. 1497–1500, December 1991.

[30] K. Walus, F. Karim, and A. Ivanov, "Architecture for an external input into a molecular qca circuit," *Journal of Computational Electronics*, vol. 8, no. 1, pp. 35–42, March 2009.

[31] A. Pulimeno, M. Graziano, D. Demarchi, and G. Piccinini, "Towards a molecular qca wire: simulation of write-in and read-out systems," *Solid State Electron.*, vol. 77, pp. 101–107, 2012.

[32] T. Fulton and G. Dolan, "Observation of single-electron charging effects in small tunnel junctions," *Phys. Rev. Lett.*, vol. 59, pp. 109–112, 1987.

[33] S. Hile, M. House, E. Peretz, J. Verduijn, D. Widmann, T. Kobayashi, S. Rogge, and M. Simmons, "Radio frequency reflectometry and charge sensing of a precision placed donor in silicon," *Appl. Phys. Lett.*, vol. 107, 2015.

[34] G. Karbasian, A. Orlov, A. Mukasyan, and G. Snider, "Single-electron transistors featuring silicon nitride tunnel barriers prepared by atomic layer deposition," in *Joint International EUROSOI Workshop and In-*

ternational Conference on Ultimate Integration on Silicon (EUROSOI-ULIS), 2016, pp. 32–25.

[35] E. Blair, *Electric-field Inputs for Molecular Quantum-dot Cellular Automata Circuits*, arxiv:1805.04029 [quant-ph] ed., 2018.

[36] C. Lent and P. Tougaw, "Lines of interacting quantum-dot cells: A binary wire," *J. Appl. Phys.*, vol. 74, pp. 6227–6233, 1993.